RSC Advances

REVIEW

View Article Online
View Journal | View Issue

Cite this: *RSC Adv.*, 2025, **15**, 24624

Challenges and opportunities in the application of carbon nanotubes as membrane channels to improve mass transfer to cells

Sara Yazdani, *[a] Davoud Biria*[a] and Gholamreza Pazuki [b]

The regulation and improvement of mass transfer through the living cell's membrane is of great importance in various industrial, environmental and medical applications. Designing membrane channels based on carbon nanotubes (CNTs) has been considered as a promising approach to this end because of the geometry of CNTs, their physical properties, high chemical stability, and excellent transport features. Despite their advantages, CNTs have a few problems such as their toxicity to living cells, low bioavailability in an aqueous medium and difficulties with managing their orientation within the cell membrane which should be addressed in the first place. Here, we tried to review recent studies on overcoming these challenges and critically evaluate their advances and suggestions for future research. Functionalization of CNTs with biocompatible materials has been recommended as the main solution which decreases the inherent cytotoxicity of the pristine CNTs, enhances their solubility and dispersibility in aqueous solution, and affects their orientation in the cell membrane. Molecular dynamics simulation results for the interactions of the functionalized CNTs and the cell membrane have been reviewed as well to demonstrate the effectiveness of functionalizing CNTs for membrane channel applications. Finally, we highlighted that modified CNTs with appropriate functional groups and favorable physical and geometrical conditions can be considered as an effective tool to make artificial channels in the cell membrane.

Received 26th April 2025
Accepted 7th July 2025

DOI: 10.1039/d5ra02939b

rsc.li/rsc-advances

1. Introduction

Plasma membrane which mainly consists of a phospholipid bilayer is a common component of all cells. It is a semi-permeable barrier that separates the internal parts of the cell from the external environment and has several crucial functions.[1] For example, the cell membrane protects the sensitive parts, maintains a favorable constant environment inside, and transfers the nutrient materials and toxic substances across the cell. In addition, there are proteins located on the surface of the plasma membrane which enables the interaction of the cell with the environment.[2]

Monitoring and controlling the transfer of materials across the cell membrane is essential for many bioengineering applications. For instance, the successful secretion of internal metabolites can intensify the bio-production of these substances, the uptake of contaminants is significant for environmental processes and the effective transfer of several drugs (doxorubicin, paclitaxel, and docetaxel) through the cell membrane is one of the most important issues in biomedicine and drug delivery.[3–6] Endocytosis, including its subtypes pinocytosis and receptor-mediated uptake, along with direct uptake, are mechanisms by which substances enter the cell. However, the hydrophobic ingredients are harder to pass through the membrane due to poor water solubility, and hydrophobicity is known as the principal factor in determining the permeability of the cell membrane.[7] Therefore, several solutions (*e.g.*, employing surfactants, peptides and nano-structures) have been suggested to overcome the lower rate of transport of hydrophobic materials to the cells. Surfactants can encapsulate the oily materials in form of emulsion droplets and facilitate their entrance to the cells by merging to the cell membrane through a pinocytosis like mechanism. However, the interactions between the surfactant and the enclosed material should be studied in detail. Application of cell-penetrating peptides can be considered as another method to facilitate the transport of hydrophobic substances to the cells.[8,9] These peptides can improve the cellular absorption of a variety of molecular cargo such as proteins, small interfering RNA (siRNA), deoxyribonucleic acid (DNA), and pharmaceuticals to various cell lines. However, their clinical application has been restricted because of the lack of cell selectivity.[10,11] Nanotechnology has provided useful tools to overcome the obstacles of hydrophobic substances entering to the cell.[12] The nano-structures act as carriers which can penetrate the membrane and transfer the

[a]*Department of Chemical Engineering, University of Isfahan, Isfahan 8174673441, Iran. E-mail: s.yazdani@eng.ui.ac.ir; d.biria@ast.ui.ac.ir*

[b]*Department of Chemical Engineering, Amirkabir University of Technology, Tehran, Iran*

desired materials binding to their bodies to the cells. The nanostructures surfaces should be modified or functionalized to activate the receptor-mediated absorption as their entry mechanism. Fig. 1 shows the nanoparticles critical sizes and the corresponding mechanisms involved in their cellular uptake, transport, and accumulation. In fact, the cellular uptake, transport, and bioaccumulation will be affected by the engineered nanomaterials (ENMs) physical properties such as geometry, aspect ratio, dissolvability, degradability and surface area. If the size and surface properties of ENMs are well designed (on the scale of a nanometer), direct bilayer penetration independent of endocytosis will occur.[13,14] Particles with larger size or high-density cationic surfaces may cause the production of cavities in the membrane, so cytotoxicity effects will be inevitable. ENMs that adsorb *via* endocytosis-mediated internalization are limited by the endocytotic size (Fig. 1).

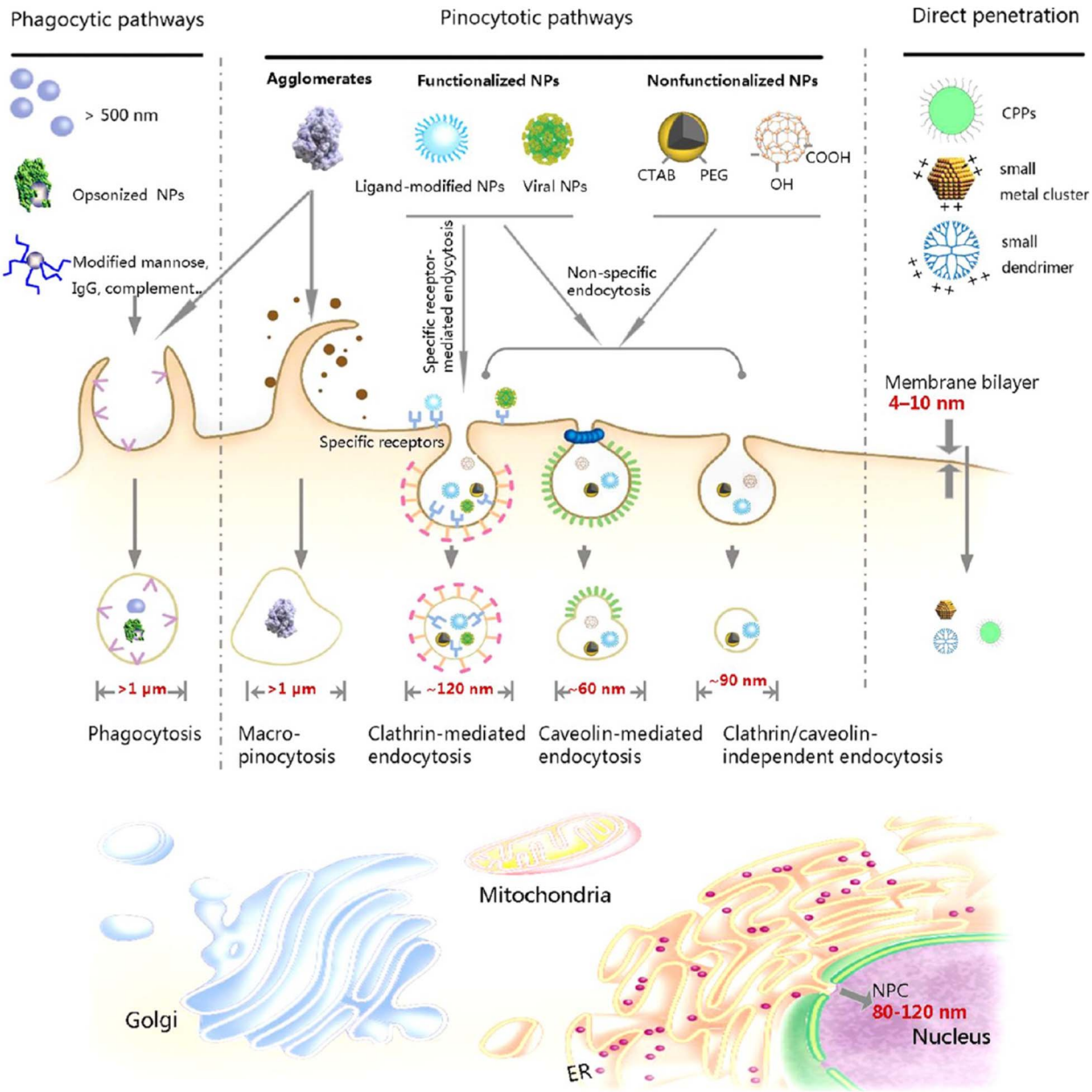

Fig. 1 Natural size rules and gatekeepers within a mammalian cell. The thickness of membrane bilayer is typically between 4 to 10 nm. The diameter of nuclear pore complex is approximately 80–120 nm.[20] The sizes of endocytic vesicles in both phagocytosis and pinocytosis pathways for nanoparticle internalization were also introduced.[21] Phagocytes could take up large particles (or nanoparticle aggragates), opsonized nanoparticles, or nanoparticles with certain liagnd modification *via* phagocytosis. Nanoparticle internalization in a nonphagocytic mammalian cell is mainly through pinocytosis or direct penetration. With various surface modifications, nanoparticles may be taken up *via* specific or nonspecific endocytosis. MR, mannose receptor; PRRs, pattern-recognition receptors; FcγR, immunoglobulin Fcγ receptor; CR, complement receptor; CPPs, cell-penetrating peptides; IgG, immunoglobulin G; ER, endoplasmic reticulum; Golgi, Golgi apparatus. Figure reprinted with permission from ref. 14. Copyright 2013, American Chemical Society.

Clathrin-coated vesicles with a 120 nm diameter are suitable for ligand-modified nanoparticles internalization.[14]

Aside from being used as shuttles for transporting compounds across the cell membrane, nanostructures such as CNTs can be employed to make channels within the cell membrane to facilitate the transport of certain materials. These channels can mimic the function of porins in the membrane and considered to be operational in a longer time than the nano-carriers. In fact, CNTs have several favorable characteristics such as high mechanical strength, electrical conductivity, chemical, and thermal stability which represent them as a proper option to modify the membranes in applications like water treatment, anti-biofouling membranes, electrical-conductive membrane, proton exchange membranes in fuel cells, and salt rejection.[15,16] Despite the appropriate functionality of CNTs in the conventional membrane systems, their application to the cell membrane can be more complex. For example, the toxicity of CNTs to the living cells should be noted at the first place. The alignment of CNTs in the cell membrane should be perpendicular to the membrane plane which is a crucial parameter to determine the effectiveness of CNTs as the porin like structures.[17–19] Finally, the selective transport of chemicals through the CNT channels is another important issue which is largely affected by the up-taking mechanism of the CNTs. Although the mentioned problems seem to be interdisciplinary, most of them can be addressed by tuning the characteristics of CNTs. Several parameters such as the physical structure, size, surface properties and functional groups of the CNTs have been considered to be effective on their performance in transporting materials across the cell membrane. Consequently, an attempt is made to review the mentioned parameters and their effects on the effectiveness of CNTs as porins for transportation of materials across the cell membrane in this paper.

2. Structure and characteristics of CNTs as transportation facilitating tools

CNTs are an allotropic form of carbon that has a cylindrical structure and is composed of sp^2 hybridized carbon atoms with a hexagonal arrangement and a C–C bond length of 1.48 Å.[22] CNTs are formed by rolling one or more graphite sheets and creating cylindrical shapes. In addition to the sp^2 hybridization, there are a few carbon bonds with sp^3 hybridization in the form of pentahedral rings in the CNTs structure which provide flexibility (*e.g.*, high bending capability) and simultaneously, facilitate the addition of functional groups to CNTs.[23,24] The most common types of CNTs are single-wall carbon nanotubes (SWCNT) and multi-wall carbon nanotubes (MWCNT). SWCNTs are composed of a cylindrical graphite layer, while MWCNTs have a more complex structure consisting of several concentrated layers of graphite.[25] While both the mentioned CNTs have found applications in various fields of bio-engineering applications, it seems that the SWCNTs are more appropriate options for mass transfer and delivery usages.[26–28] SWCNTs can overcome the resistances of cell entry more conveniently resulting in higher penetration rate. The solubility, biocompatibility, tracking in biological conditions and the purity of SWCNTs are considered to be superior than MWCNTs and their characterization is simpler than MWCNTs.[26–30]

Besides to their high physical stability, CNTs have several favorable characteristics to act as a vehicle for transportation of various compounds through small interfaces like tissues and cell membranes. For instance, they have high conductivity and proper optical properties, high surface to volume ratio, the ability to possess various functional groups and bind to a plethora of pharmaceutical compounds on their internal and external surfaces.[31] However, their poor aqueous solubility and toxicity for the living cells can be considered as serious problems to their extensive application in biomedicine. Previous research works have revealed that their synthesis method, size, and surface properties are the main parameters that affect the CNTs toxicity at *in vitro* and *in vivo* scale.[32] Functionalizing the CNTs with biocompatible materials (*e.g.*, PEG, carboxylic and hydroxyl groups) has been suggested to reduce their toxicity and improve some of the surface properties such as their interfacial adhesion. The toxicity of CNTs and efforts to overcome this challenge has been assessed in the following section.

Functionalizing the CNTs can be advantageous to several other properties of these nano structures. It has been reported that the functionalized CNTs can easily pass through the cell membranes and distribute in various cell parts through alternative routes.[33] In fact, the modified CNTs can directly pass through the cell membrane and be transferred to the cytoplasm or penetrate into the cell through endocytosis or active phagocytotic pathways. Fig. 2 shows different cellular uptake mechanisms for CNTs. These mechanisms usually exist during cellular uptake and are strongly dependent on the type of CNT, functionalization chemistry, surface charges, hydrophobic nature of covalently linked molecules, and the cell type. The ability of CNTs to be directly transferred to the cells has opened the way for many studies that investigate the potential of these nanomaterials as drug carriers. The advancements in this subject have been recently reviewed by Lacerda *et al.*[34] and Corredor C *et al.*[17] Ghoderao *et al.*[35] developed a multifunctional nanovector by conjugating doxycycline (Doxy) with Fe_3O_4 nanoparticle-decorated multiwalled carbon nanotubes (MWCNTs), forming doxycycline-MWCNTs/Fe_3O_4 hybrids to enhance drug delivery performance.[35] Their system exhibited superparamagnetic behavior, improved doxy loading and stability, and significantly enhanced antibacterial activity against *E. coli* and *B. subtilis* at lower drug concentrations. The conjugates also showed sustained drug release and higher bioavailability due to magnetically guided uptake, offering a promising strategy for targeted, controlled antibiotic delivery.[35] Tan *et al.*[36] developed four types of biopolymer-coated, betulinic acid-loaded MWCNT nanocomposites—MWBA-CS (chitosan), MWBA-PG (PEG), MWBA-T2 (Tween 20), and MWBA-T8 (Tween 80)—to enhance CNT biocompatibility for drug delivery applications.[36] David *et al.* [37] synthesized TiO_2 nanoparticle-decorated multi-walled carbon nanotubes (MWCNTs) and embedded them into cellulose acetate–collagen films to develop novel antimicrobial and

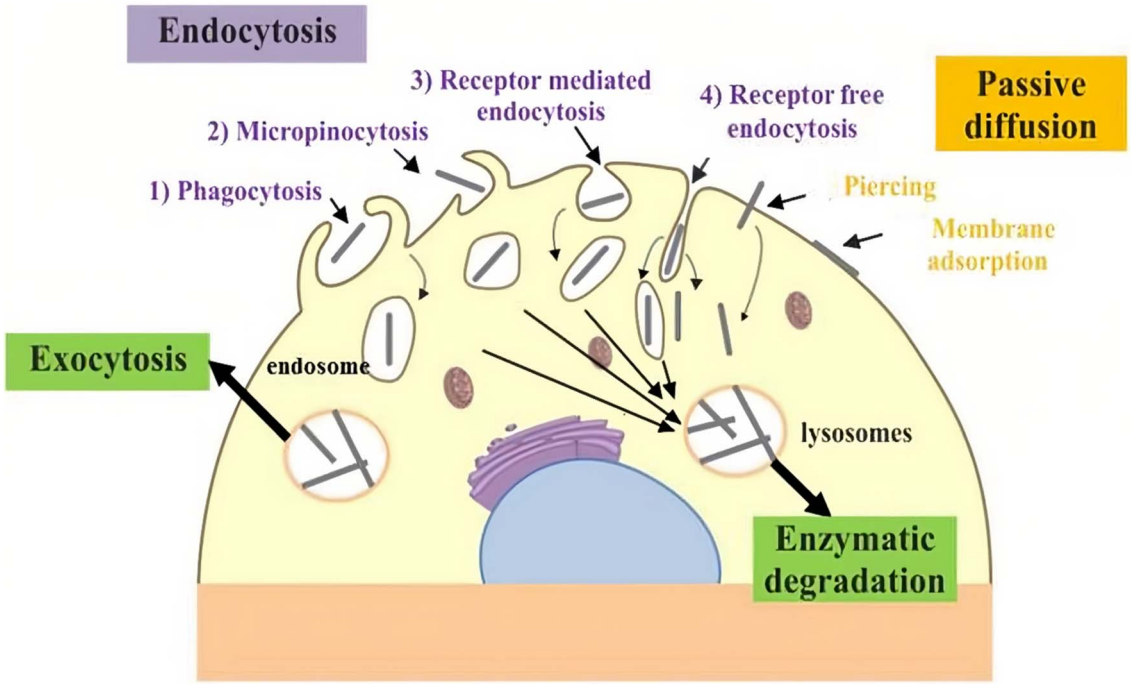

Fig. 2 Different cellular uptake mechanisms for CNTs (reproduced from ref. 40).

biocompatible wound dressing materials.[37] Khalid *et al.* [38] reinforced bacterial cellulose (BC) films with multiwalled carbon nanotubes (MWCNTs) to develop a composite material for diabetic wound healing applications. The BC-MWCNT composite exhibited broad-spectrum antibacterial activity and significantly accelerated wound closure in diabetic rats (99% healing *vs.* 77% in controls after 21 days). Histological and molecular analyses confirmed enhanced re-epithelialization and reduced expression of pro-inflammatory cytokines (IL-1α, TNF-α), alongside increased VEGF expression, indicating a favorable immunomodulatory and regenerative environment.[38] Beyond their application as drug transporters, CNTs can be used to form nano pores in the cell membrane to control the transportation of various molecules through the cells.[29] Apart from the type, size, toxicity and surface properties, the orientation of CNTs within the cell membrane can be considered as a crucial parameter influencing the successful application of CNTs as synthetic nano channels in the cell membrane.[39] This orientation is also depended on the structure and functional groups of the CNTs and reviewed in the next sections.[39]

3. The challenge of toxicity bioavailability of CNTs

The high toxicity and low aqueous solubility of CNTs are their main limitations for biomedical applications. Due to their highly hydrophobic surface structures, CNTs exhibit very low solubility in most solvents, both organic and inorganic. Enhancing the solubility of CNTs in aqueous solutions is essential for their application in biological systems. Additionally, it is important to address the inherent toxicity of CNTs. This can be achieved by modifying their surfaces with materials that improve their physicochemical properties. Functionalizing CNTs with organic and inorganic materials can enhance their dispersion, boost their biocompatibility, and reduce their toxicity. The structure, utilized synthesis method, presence of surfactants, modification by functional groups, and catalyst impurities are among the important factors that can considerably affect the toxicity and solubility of CNT.[28] Functionalizing CNTs is a pivotal strategy to reduce their toxicity and enhance their solubility, thereby making them more suitable for biological applications. There are two principal methods for functionalizing CNTs: covalent and non-covalent functionalization. Covalent functionalization involves chemically bonding functional groups to the CNT surface, which can significantly alter their intrinsic properties. This method typically leads to improved solubility and reduced toxicity as it introduces hydrophilic groups that enhance dispersion in aqueous solutions.[41] On the other hand, non-covalent functionalization relies on physical interactions, such as π–π stacking, van der Waals forces, and electrostatic interactions, to attach functional molecules to the CNTs without altering their core structure. This method preserves the inherent electrical and mechanical properties of CNTs while still enhancing their solubility and biocompatibility. Both functionalization techniques are crucial in tailoring the properties of CNTs to meet specific requirements in various biomedical and industrial applications.[28,42]

Although the mentioned factors have a similar final influence on living cells, their destructive function are not identical. The fatal interaction of CNTs with the cells has been explained by three major mechanisms.[32,43] The first mechanism is based on the irrecoverable mechanical damage to the cellular/nuclear

membrane.[43] Endocytosis, phagocytosis, and nano-scale penetration are the main routes for entering the nanostructures to a lipid membrane, which strongly depends on the dimensions of CNTs, especially their length. The ability of CNTs to penetrate macrophage membranes and trigger an immune response is significantly influenced by their length and shape. Studies have shown that shorter CNTs, around 0.22 μm in length, are more readily absorbed by macrophages and phagocytes than longer CNTs, which are greater than 0.8 μm in length.[44,45] In experiments conducted on rats, it was found that four weeks after injection into subcutaneous tissue, the majority of the short CNTs were present within the cytosol of macrophages. Conversely, the longer CNTs remained free-floating, leading to persistent inflammation.[46] Oxidative stress is the second toxic mechanism that happens due to high level of reactive oxygen species (ROS) in CNTs structure and leads to multiple negative side effects in the cell such as apoptosis, necrosis, proliferation reduction, oxidative DNA damage, and inhibition of cell growth.[47,48] The genotoxicity mechanism is the last one, somehow related to DNA damages specified by a wide spectrum including the interaction between CNTs and proteins taking part in chromosome aberration, the effect of CNT on the mitotic spindle, complex DNA oxidation, DNA failure.[32,43] Functionalizing CNTs with certain biocompatible and biodegradable materials, modifying the CNT surfaces with special metal oxides, and conjugating with proper proteins have been suggested to address the toxicity problem. In addition to toxicity reduction, these methods can improve CNTs' dispersibility in aqueous solutions and also help to control the alignment of CNTs within the cell membrane. Moreover, the same methods have been applied to convert the CNTs to intelligent delivery agents which enables them to have the multi-responsiveness property.[28,49] Addition of functional groups to CNTs can be carried out either covalently or non-covalently. The involving carbons hybridization structure changes from sp^2 to sp^3 state after covalent binding to the desired functional groups of the reactive molecules. Fluorination of CNTs, carbene and nitrene addition, cycloaddition, cholorination, and bromination are a few examples of functionalizing CNTs covalently. On the other hand, a typical non-covalent functionalization process includes ultrasonication of CNTs, centrifugation and finally filtration.[28] Ultrasonication, which involves using ultrasonic waves to disperse CNTs in a solvent. This process helps to break up aggregates and ensure that the CNTs are evenly distributed. Surfactants or polymers are often added during ultrasonication to stabilize the dispersed CNTs through non-covalent interactions. The energy from the ultrasonic waves facilitates the adsorption of these stabilizing agents onto the CNT surfaces, enhancing their solubility and preventing re-aggregation. In next stage, the mixture is subjected to centrifugation. This step separates the well-dispersed, functionalized CNTs from any remaining large aggregates or unfunctionalized CNTs. During centrifugation, the centrifugal force causes the denser, unmodified aggregates to settle at the bottom of the centrifuge tube, while the stabilized, functionalized CNTs remain in the supernatant. This process helps to purify the CNTs, ensuring that only those that have been effectively functionalized and dispersed are retained. The final step is filtration, which further purifies the functionalized CNTs. The supernatant from the centrifugation step is passed through a filter, typically made of a membrane with pores small enough to retain the CNTs but large enough to allow the solvent and any unbound functional agents to pass through. This stage removes any residual impurities and unadsorbed functional molecules, resulting in a purified solution of non-covalently functionalized CNTs.[50–52] A broad range of compounds such as bio-molecules, polymers, surfactants, and poly nuclear aromatic compound can be attached to the surface of CNTs through physical weak interaction in the non-covalent process.[51,53]

Studying the toxicity of CNTs on various cells and the effect of their modification by adding the proper functional groups has been frequently reported in the literature. Results of several recent researches on this topic have been summarized in Table 1. The Table 1 provides a detailed summary of studies investigating the cytotoxic effects of MWCNTs and SWCNTs on various cell types. These studies utilize a range of cytotoxicity assays, including CCK8, LDH, MTT, MTS, Trypan blue, Flow cytometry, and CellTiter-Glo, with the CCK8 assay being the most frequently employed method. The administered doses vary widely from 0.1 μg mL^{-1} to 400 μg mL^{-1}, reflecting differences in experimental designs and the sensitivity of the cell types tested. Cell viability percentages range from as low as 30% to as high as 100%, typically correlating with higher doses or more sensitive cell types showing lower viability. A broad spectrum of cell types, including HepG2, NIH-3T3, Met-5A, Raw264.7, HEK293, HUVECs, HT29, A549, HeLa, and primary cells, have been examined, with both human and murine cell lines represented. The studies span from 2016 to 2024, indicating ongoing research interest in this area. Comparatively, MWCNT studies generally reveal a more consistent trend of reduced cell viability at higher doses. For instance, MWCNT at 400 μg mL^{-1} shows less than 50% viability in Raw264.7 cells.[54] Conversely, moderate doses of MWCNT at 64 μg mL^{-1} result in about 60–80% viability across various cell types including HUVECs,[55] THP-1,[56] and SMCs.[57] In contrast, low doses of SWCNT at 5–40 μg mL^{-1} exhibit less than 70% viability in human neuronal cell line LN18.58 Cell type sensitivity also varies, with A549 cells showing only 30% viability at 50 μg mL^{-1} of MWCNT,[59] while hMSCs exhibit 100% viability at 20 μg mL^{-1} of SWCNT.[60] Yearly trends suggest that earlier studies often employed higher doses with lower viability outcomes, whereas recent studies focus on specific cell lines and slightly lower doses, yielding varied results. The type of assay used impacts the observed cell viability, highlighting the necessity for multiple assays to validate findings. Overall, MWCNTs demonstrate consistent cytotoxic effects at higher doses, whereas SWCNTs show more variable results, influenced by the type of cytotoxicity assay and the cell type. As it can be estimated from Table 1 and in order to have a high cell viability percentage (80 <), CNT dose less than 100 μg mL^{-1} is preferred. In addition to the dose of CNT, other parameters such as diameter of CNT, size distribution, surface chemistry, and various functional groups (hydroxylated CNT, carboxylated CNT) can affect the cell viability. For instance, Zhao *et al.*[61] studied the effect of various diameters of CNTs on

Table 1 Cytotoxicity studies on pristine and functionalized CNTs with various cell types

Type of CNT	Functional groups	Cytotoxic test	Dose	% Viable cells	Cell type	Year, ref
MWCNT	Pristine, hydroxylated, carboxylated	CCK8	40 μg mL^{-1}	50	HepG2	2016 (ref. 74)
MWCNT	Carboxylated	CCK8	100 μg mL^{-1}	80 <	NIH-3T3	2016 (ref. 75)
MWCNT	Pristine	LDH	80 μg mL^{-1}	80	Met-5A	2016 (ref. 76)
MWCNT	Oxidized-MWCNT	MTS	400 μg mL^{-1}	50 <	Raw264.7	2016 (ref. 54)
SWCNT	Pristine, hydroxylated, carboxylated	CellTiter-Glo	—	—	HEK293, MCF10A, MRC-5, HepG2	2017 (ref. 77)
MWCNT	Pristine	LDH, WST8	32 μg mL^{-1}	~80	HUVECs	2017 (ref. 78)
MWCNT	Oxidized	MTT	200 μg mL^{-1}	40	HT29	2017 (ref. 79)
MWCNT	Pristine, carboxylated	PI	50 μg mL^{-1}	30% dead	A549	2017 (ref. 59)
SWCNT	Carboxylated	CCK8	50 μg mL^{-1}	~50	HUVECs	2018 (ref. 80)
SWCNT	Carboxylated	CCK8	50 μg mL^{-1}	~60	HUVECs	2018 (ref. 81)
SWCNT	Pristine	LDH	2 μg mL^{-1}	50	HeLa, HUVEC, Hep2G	2018 (ref. 82)
MWCNT	Pristine	Trypan blue	60 μg mL^{-1}	60 <	Primary microglial cells	2018 (ref. 83)
MWCNT	Oxidized	CCK8	60 μg mL^{-1}	~80	HUVECs	2019 (ref. 55)
MWCNT	Pristine, hydroxylated, carboxylated	CCK8	64 μg mL^{-1}	80 <	THP-1	2019 (ref. 56)
MWCNT	Pristine	CCK8	64 μg mL^{-1}	60 <	HUVECs	2019 (ref. 61)
MWCNT	Pristine, carboxylated	CCK8	64 μg mL^{-1}	60 <	SMCs smooth muscle cells	2019 (ref. 57)
MWCNT	Hydroxylated, carboxylated	CCK8	64 μg mL^{-1}	60 <	HUVECs	2019 (ref. 84)
MWCNT	Pristine	LDH, trypan blue	12 μg mL^{-1}	60 <	Bronchial epithelial primary cells	2019 (ref. 85)
SWCNT, MWCNT	Carboxylated	PI, acridine orange	50 μg mL^{-1}	80 <	H1299	2019 (ref. 86)
SWCNT	Carboxylated	WST1	20 μg mL^{-1}	100	hMSCs	2019 (ref. 60)
MWCNT	Pristine, acid functionalized, and annealed treatment	Flow cytometry	120 μg mL^{-1}	~50	Raw264.7	2020 (ref. 87)
MWCNT	Pristine	LDH	—	—	Mesothelial LP9	2020 (ref. 88)
MWCNT	Pristine, carboxylated	MTT, LDH	—	—	A549	2020 (ref. 89)
SWCNT	Pristine	MTT, LDH, trypan blue	50 μg mL^{-1}	80 <	Human umbillical cord MSCs	2020 (ref. 90)
MWCNT (+fibers)	Pristine	WST1	24 μg mL^{-1}	60 <	BEAS2B	2020 (ref. 91)
MWCNT	Pristine, oxidized				Hep2G	2022 (ref. 92)
SWCNT	Pristine, carboxylated	Trypan blue, MTT	5–40 μg mL^{-1}	70 <	Human neuronal cell line LN18	2022 (ref. 58)
SWCNT	Pristine, carboxylated, aminated	CCK8	37.5 μg mL^{-1}	~75	HEK 293	2022 (ref. 64)
MWCNT	Pristine	CCK8	64 μg mL^{-1}	~60	HUVECs	2022 (ref. 32)
MWCNT	Pristine, carboxylated	Trypan blue, MTT, and live dead cell assays	5–40 μg mL^{-1}	~70	LN18	2023 (ref. 93)

their toxicity to human umbilical vein endothelial cells and concluded that the MWCNT with small diameters had the highest level of cytotoxicity at a constant mass concentration. This was justified by the fact that the human endothelial cells may be affected by the autophagy dysfunction and endoplasmic reticulum stress caused by the small diameter of CNTs.[61] Jiang *et al.*[62] evaluated the role of lengths, functional groups, and electronic structure on cytotoxicity of SWCNT. They concluded that SWCNTs with longer length has lower toxicity than those with shorter length. They also showed that semiconducting SWCNT and metallic SWCNT had minimum and maximum toxicity levels, respectively. Moreover, their results indicated that the carboxylated SWCNT derived a grosser toxicity than the hydroxylated SWCNT especially in terms of genotoxicity. Chowdhry *et al.*[63] compared the cellular toxicity of pure MWCNT, carboxy MWCNT, and amino MWCNT on HEK293 cells and zebra fish *in vivo* by MTT assay and trypan blue. The results showed the toxicity increased at higher concentration of MWCNT and unmodified MWCNT had the highest level of toxicity in all concentrations compare to functionalized MWCNT. The cell viability for carboxy MWCNT was higher than amino MWCNT at 25 μg mL^{-1}.[63] Yazdani *et al.*[64] evaluated the toxicity of CNTs before and after modification by 1,2-distearoyl-*sn*-glycero-3-phosphoethanolamine-*N*-[carboxy(polyethylene

glycol)] (DSPE-PEG-COOH) and also after adding ethylenediamine on HEK-293 cells. The CCK8 assay results showed the cell viability of modified CNTs was higher than pristine CNTs in all concentrations. They concluded the CNT functionalization lead to decreasing their toxicity and also improve dispersibility and aqueous solubility.[64] Despite numerous advancements in improving the biocompatibility and reducing the toxicity of CNTs, significant regulatory challenges remain before their clinical translation can be realized. One of the major barriers is the lack of universally accepted standards for evaluating the toxicity of nanomaterials, including CNTs.[65,66] Currently, testing protocols vary across studies, making it difficult to compare results and assess safety consistently. Regulatory agencies such as the FDA and EMA emphasize the need for comprehensive risk assessments, including long-term toxicity, biodistribution, immunogenicity, and biodegradability.[67,68] Moreover, mitigation strategies such as surface functionalization with FDA-approved polymers (*e.g.*, PEGylation),[69] control over size and aspect ratio, and removal of catalytic impurities are key to improving biosafety.[70,71] Development of biodegradable CNT derivatives and targeted delivery systems also helps to minimize side effects and reduce systemic toxicity.[72] In this context, an integrated approach that combines advanced functionalization techniques, standardized testing, and regulatory alignment is essential to accelerate the safe and effective clinical translation of CNT-based systems.[72,73]

4. Interactions between CNTs and the cell membrane

Among the diverse mechanisms for uptake of nanostructures by living cells (*i.e.*, direct uptake, endocytosis, phagocytosis, and receptor-mediated endocytosis), the most effective internalization mechanism is known to be receptor-mediated endocytosis, which is controlled by various parameters such as the size,[94,95] geometries,[96–99] elastic stiffness,[100,101] and surface properties of the nano structures. The nano structure geometries have attracted much attention, because of the different shapes of nanostructures such as nano-capsules, nanorods, and nanosheets that have different interactions with cell membranes. Experiments and simulation results showed that the nanostructures with irregular geometry tend to rotation.[102] For instance, one-dimensional nanomaterials may enter cells by the "head diagnosis and rotation" mode. In this state, the uptake happens by the rotation of the nanostructures to the near-vertical alignment.[102] Molecular dynamic simulation (MDS) results indicated that the endocytosis takes *via* a laying-down and then standing-up rotation for nanostructures with a sphere-cylindrical shape.[103] Besides, it has been identified that the direction and rotation of the nanostructures are of major biological importance.[102] The cellular uptake of CNTs functionalized with biocompatible materials is influenced by multiple factors, including cell type, surface functional groups, and the physical characteristics of CNTs such as length and diameter.[104–106] Studies have shown that shorter CNTs, especially those with amino functionalization, can behave like tiny nanoneedles capable of passive membrane penetration. However, differences in cell membrane composition and surface receptor expression also play a significant role in determining uptake efficiency.[107,108] In other cases, CNTs modified with DNA sequences, and proteins indicated an endocytotic path of penetration.[109] Raffa *et al.*[110] synthesized different type of MWCNTs and characterized their features such as size (diameter and length), metal impurity, surface chemistry, and carbon soot. The cellular uptake was investigated by standard fluorescent probes and transmission electron microscopy (TEM) images. They concluded that the length of CNT have a considerable effect on the CNT uptake and MWCNT with diameter shorter than 1 μm are penetrated easily.[110] Shen *et al.*[111] investigated the role of coating CNT on the stabilization and formation of CNT porins. Results showed that density of lipid coating and end-functionalized groups had a strong effect on the insertion of CNT into a bilayer membrane. Fig. 3 shows the insertion of CNT coated with lipid into a 1-palmitoyl-2-oleoyl-*sn*-glycero-3-phosphocoline (POPC) lipid membrane at various coating density. The angle between the CNT central axis and the lipid membrane signed θ. Fig. 3a indicates at the low coating density (surface coating density (SCD) = 0.72), the insertion angle (θ) of CNT is toward a small angle, and simultaneously lipid coating of CNT fused with the membrane. The equilibrium configurations of CNT with low density and pure CNT are the same during the simulation. When the coating density increased, the CNT would like to insert into a bilayer membrane at a vertical alignment. The angles are 78°, 83°, and 85° for CNT with coating densities 2, 4, and 5.4, respectively (Fig. 3b).[111] Final results indicated the fewer functional groups and average coating density are optimum state of efficient CNT porins. All research results showed that the enter angle of CNT into the cell membrane is not exactly 90° due to the thermal fluctuation.[111] Moreover, CNT could easily enter the membrane with an arbitrary orientation (vertically, horizontally, and tilted) before functionalized and stayed in the hydrophobic part of membrane, although it preferred to be located vertically after functionalized due to the electrostatic interactions between the head groups of membrane and functional groups on CNT's surface. Functionalized CNTs have strong potential to serve as synthesized channel with high capability. The initial structure of CNT affects the terminal orientation of CNT in the membrane and as the CNT's length increases, the rotation movement will become more complex.[39]

5. Artificial membrane channels (porins) based on CNTs application

There are proteins in the lipid bilayer of the cells membrane that formed channels called porins. Porins are open channels usually filled with aqueous phase around the outer membrane and conducts hydrophilic molecules passively thorough the channel. Various types of porins have been specified in Gram-negative bacteria and categorized according to the type of their expression, kind of activity, and operating structure.[112,113] For example, *Escherichia coli* (*E.coli*) generates three main types

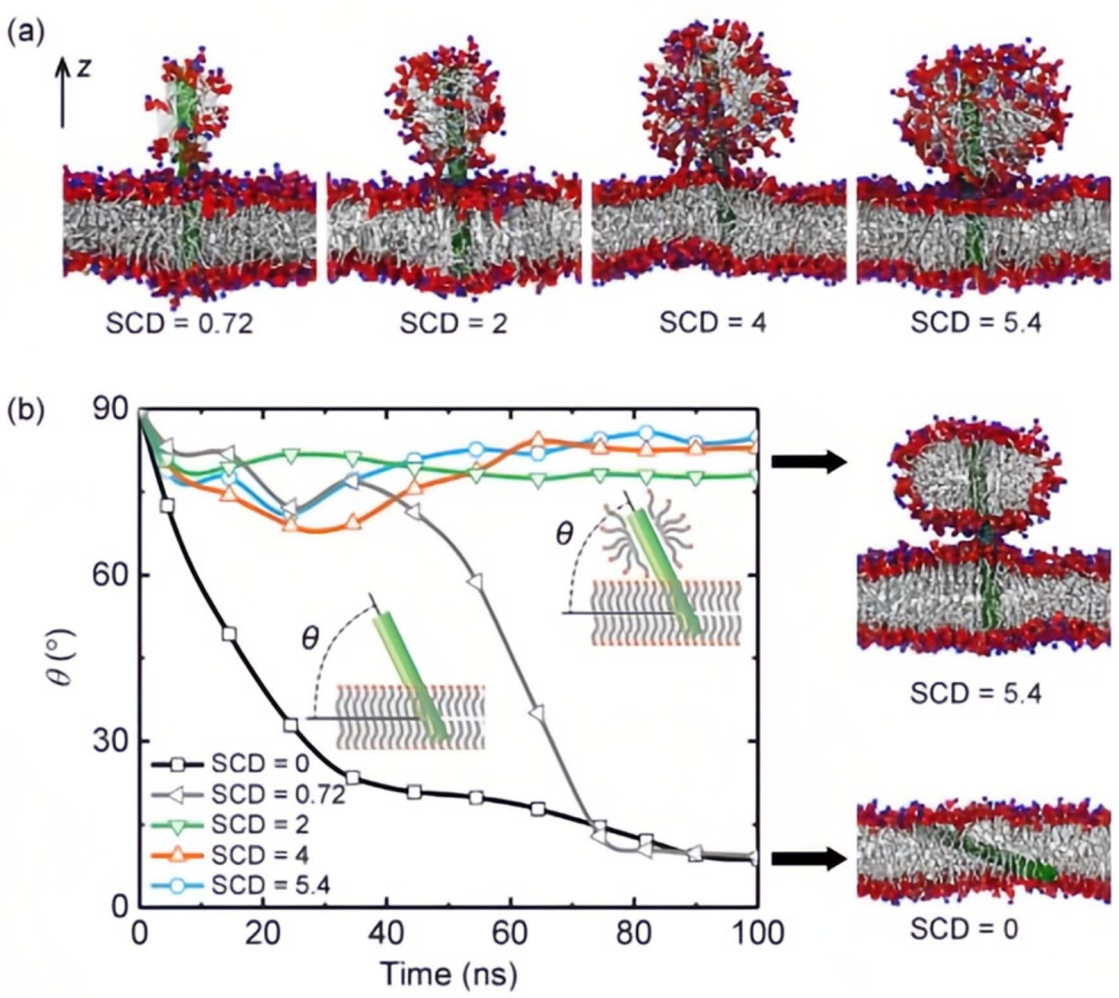

Fig. 3 Incorporation of CNTs coated with lipid into a POPC bilayer membrane. (a) Snapshots of the configurations at starting time with different SCD. (b) Time evolution of the insertion angle θ of CNTs at five SCD values (schematically shown in the insets). Right panel indicates snapshots of balance configurations for two SCD after 100 ns simulations.[111] Figure reproduced with permission from ref. 111. Copyright 2020, Elsevier.

of trimeric porins: OmpF, OmpC, and PhoE. Initial research and studies with these three porins made the basis of the recent knowledge of many other kinds of porins.[113]

Developing synthetic biological membrane channels, with smart selectivity, and high yield, similar to natural membrane channels attracts a lot of interest. The lipid bilayer as the universal base for cell membrane structure is the first barrier that CNTs face when interacting with the cells. In addition to self-assembly properties, a lipid bilayer has other properties such as fluidity and deformability, which are essential for many membrane functions. The perfect transport properties of CNTs and CNTs' thin hydrophobic inner pores made them an ideal membrane channel platform. In addition, CNTs' inner structure mimics the structural motifs of biological channels.[114] As mentioned previously, after CNT functionalized to improve their solubility and decrease toxicity, they can penetrate into lipid membranes and cell walls. CNTs with a short length have been obliged into membranes to construct sensors.[115]

CNT porins are composed of long parts between 10 to 20 nm of lipid-stabilized SWCNTs that can penetrate phospholipid membranes to create pores on a nanometer scale that is dependent on the geometry and many main transport features of biological membrane channels, such as selective permeability, gating mechanisms, rapid transport rates, directionality, regulatory factors, energy requirements, pore size and shape, and ion specificity. Evaluating the hydrophobic/hydrophilic interactions between CNTs and bacterial cell membranes, and also, investigation of the mechanical properties changes in complex system of CNTs and bacterial cell membranes is crucial to develop effective synthetic channels in the cell membrane.[116] Sullivan *et al.*[117] synthesized a group of CNT porins based on CNT with 1.5 nm diameter that mimic the structure and main motifs of membrane proteins and investigated the behavior of CNT porins in lipid membranes composed of 1,2-dioleoyl-*sn*-glycero-3-phosphocholine lipid (DOPC), and 1,2-dimyristoyl-*sn*-glycero-3-phosphocholine lipid (DMPC) by high-speed atomic force microscopy (HS-AFM) and MDS. HS-AFM results show the motion of CNT porins was diffusive in the lipid bilayer plane and diffusion coefficient for CNT porins was similar to diffusion coefficient of membrane proteins in lipid bilayers.[117] Geng

et al.[114] synthesized short CNTs from intact long CNTs through sonication-assisted cutting process in the presence of 1,2-dioleoyl-*sn*-glycero-3-phosphocholine (DOPC) lipid. Results indicated that channels with unitary conductance of 70–100 picosiemens were created under physiological conditions, while short CNTs automatically penetrated into lipid bilayers and cell wall membranes. They called these CNT channels as "CNT porins" which capable to transport DNA, protons, water, and small ions.[114] Tunuguntla *et al.*,[118] explained synthesis methods of CNT porins by long CNTs in presence of lipid amphiphiles through ultrasound-assisted cutting process and evaluated the incorporation of carbon nanotube porins (CNTP) with lipid membrane through a proton permeability assay.[119] They also evaluated methods for measuring the conductance of single CNT porins in lipid bilayers, and plasma membranes. Results showed the CNTPs generated by this cutting method stay stable and active for about three months.[118]

Liu *et al.*[120] investigated the antimicrobial properties of CNTs and their mechanisms of action against microorganisms for water disinfection and microbial control. They reported that cell membrane damage and release of intracellular contents as a possible mechanism led to bacterial cell death. CNTs attachment to the bacterial cells changed the structure, permeability and proton motive force of the cells membrane.[120] Pérez-Luna *et al.*[116] studied the hydrophobic/hydrophilic interactions between pure and functionalized MWCNTs with giant unilamellar vesicles (GUVs) as a simple model of cell membranes as well as the mechanical properties changes of the system and concluded that the interactions between MWCNTs with cell membranes depended on the type of CNT functionalization (Fig. 4). Oxidized MWCNTs (ox-MWCNTs) had an interaction with the polar section of phospholipids and remained in the cell membrane, and alkyl functionalized MWCNTs (alk-MWCNTs) remained inside the cell membrane. The mechanical features of complexes systems investigated *via* the electrode deformation method and the results showed that alkyl-MWCNTs formed stable complex structures inside the membrane.[116] Li *et al.*[121] measured the amount of water and chloride ion penetration through CNT porins with 0.8 nm diameter by using fluorescence-based assays under optimum experimental conditions.

6. Molecular dynamic simulation analysis for studying CNT based porins

Recently, MDS has been applied to investigate the interactions between nano structures such as CNTs and phospholipid

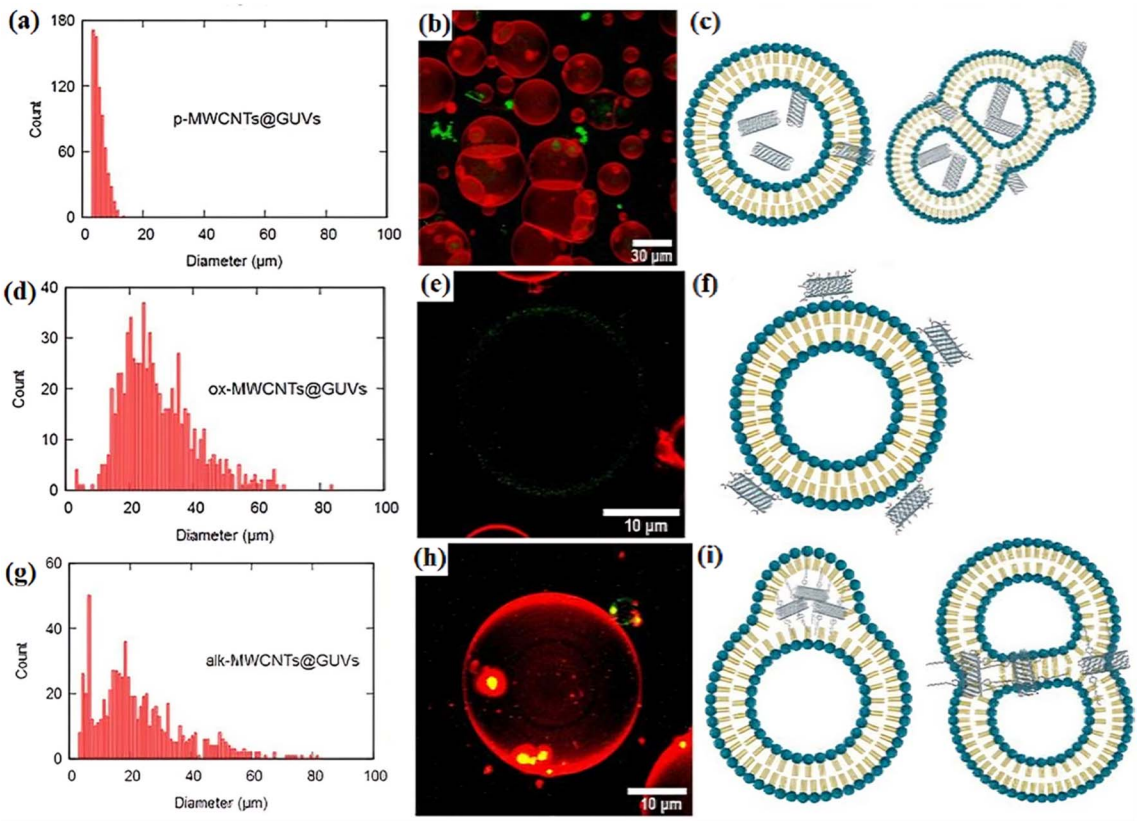

Fig. 4 (a) Diameter histogram of *p*-MWCNTs@GUVs at a 2 μg mL^{-1} concentration of CNTs, (b) confocal images of *p*-MWCNTs@GUVs at a 2 μg mL^{-1} concentration, (c) cartoon of the interaction in the *p*-MWCNTs@GUVs systems, (d) diameter histogram of oxMWCNTs@GUVs at the concentration of 2 μg mL^{-1} of CNTs after one hour of incubation, (e) confocal images of ox-MWCNTs@GUVs at 2 μg mL^{-1}, (f) cartoon of the interaction of the system ox-MWCNTs@GUVs, (g) diameter histogram of alk-MWCNTs@GUVs at a 2 μg mL^{-1} concentration of alk-MWCNTs, (h) confocal images of alk-MWCNTs@GUVs at a 2 μg mL^{-1} CNTs concentration, colocalization of alk-MWCNTs GUVs on "ghost-like" structures, and (i) confocal images of alk-MWCNTs@GUVs at a 2 μg mL^{-1} CNTs concentration, colocalization of alk-MWCNTs GUVs on "ghost-like" structures. Figure reprinted with permission from ref. 116. Copyright 2018, Springer Nature.

membranes.[122] Simulations indicated that CNTs with a length analogous to the thickness of a lipid bilayer membrane can automatically cross over the cell membrane.[114] How the CNTs come down, conjugate to, and translocate through cell membranes can be studied by MDS.[34] It is important to note that in many coarse-grained force field-based molecular dynamics simulations,[123] the polarizability of CNTs is often not explicitly considered, and carbon atoms are typically modeled as Lennard-Jones particles with zero partial charges. However, atomistic simulations frequently include partial charges and more detailed parameterizations to capture interactions more accurately, as exemplified by Vögele *et al.*[124] developed an AMBER- and Lipid14-compatible parameterization scheme for CNTs embedded in lipid membranes. One of the pioneering MDS results of the interaction of CNT with the membrane showed that SWCNT with hydrophilic groups at the open ends was capable of displacement in the membrane spontaneously which could form a transmembrane channel permeable for water molecules.[125] Zimmerli *et al.*[126] evaluated the formation and transport features of CNT-based transmembrane channels by using MDS. Feasibility of electrophoretic transport of short RNA segments through a channel based on transmembrane SWCNT was observed. Results indicated that a partial electrostatic potential difference (1–2 V) retained the RNA part transposition with a velocity of about 1–30 nucleotides per nanosecond (ns).[126] Studying the interactions of the membrane with pure CNTs of various lengths indicated that CNTs with shorter lengths inside the lipid bilayer, preferred to be oriented parallel to lipid molecules. On the other hand, CNTs with longer lengths oriented parallel to the membrane plane.[127] Computation results of a single chain mean field theory (SCMF)[128] determined that the necessary penetration energy for a vertically oriented CNT with a hydrophilic surface is about a hundred of k_BT.[129] A vertical penetration possesses the minimum energy obstacle and generates the minimum damage to the membrane. The hydrophobic core of the bilayer adsorbs CNTs with a hydrophobic surface, which slows down their motion and prevents them to separate from the membrane. The SCMF theory was also used to evaluate the penetration parameters of a CNT that was modified with hydrophilic and hydrophobic bands on its surface.[130] It was shown that a particular pattern on the surface of a CNT can simplify its permeation through a lipid bilayer.[131] Kraszewski *et al.*[132] evaluated the interactions of pure and functionalized SWCNTs with the membrane *via* MDS. Results of MDS simulations indicated that pure SWCNT independently penetrated into the bilayer. A multi stage procedure was suggested which included an initial landing and floating on the bilayer surface, penetrating quickly from the head groups in the next step, and finally moving smoothly through the lipid tails zone.[132] It has been reported that during the amine modified SWCNTs translocation, amine groups were deprotonated on the membrane surface in the simulation and afterward, when CNT came close to the opposite membrane side, the charges were retrieved.[132] The MDS for penetration of open and closed SWCNTs to the lipid membrane through the all-atom model were also investigated.[133] The penetration of CNT with a closed-end brings smaller membrane disorders than CNT with an open end. A closed SWCNT has a minimum free energy obstacle to penetration through the membrane, which makes it a favored choice for drug delivery, performing as nano-carriers.[133] In order to explore the properties of cell membrane interactions with pure and modified SWCNTs of various diameters, lengths, and functional groups locations, simulations with closed SWCNTs and aggregates of SWCNTs had been performed.[134] The CNTs had various locations of hydrophilic groups: SWCNTs with a complete hydrophilic surface, with hydrophilic end groups, and a complete hydrophobic surface. Simulation results showed the small CNTs automatically penetrated the membrane. The membrane center was the location where the hydrophobic SWCNTs were in the maximum stable state. When the length of CNTs was shorter than the membrane thickness, the least free energy level for the vertical direction in the bilayer was a little lower.[134] SWCNTs with a modified hydrophilic surface were ideally adsorbed by the membrane at the interface of water and lipid and the orientation of SWCNT was parallel to the membrane plane. The possibility of crossing the membrane for such SWCNTs is extremely low. Kraszewski *et al.*[135] evaluated the internalization of modified CNTs into a lipid bilayer *via* MDS (using NAMD2.7b2) and Monte Carlo simulations as a function of the CNTs length. They concluded that hydrophobicity played an important role in the insertion process.[135] Tabari *et al.*[136] investigated the interactions between CNTs and cell membranes using MDS (NAMD and GAUSSIAN package) and density functional theory (DFT) models. DFT results indicated that for open-ended CNTs, there were unsaturated bonds at the end of the tubes and also a significant dipole moment that should not be neglected. They first determined the partial charges for pure and modified CNTs using DFT and then applied the obtained results to the molecular dynamic force field.[136] DFT results showed that partial charges for functionalized CNTs were higher than pure CNT, and MDS results showed that the interaction energy of nanotubes with biological membrane was very strong.[136] Gao *et al.*[39] investigated the orientation and permeation of pure and modified CNTs in a lipid bilayer through atomic MDS. Results showed that pure CNTs could eagerly penetrate into the membrane and settle in the hydrophobic part without particular orientation (Fig. 5a), while modified CNTs stand upright in the lipid bilayer center (Fig. 5d and e).[39] Pure CNT was preferred to be located with an oblique angle of approximately 30° (Fig. 5b), while the functionalized CNT preferably was placed vertically during the whole simulation time in both horizontal and vertical entering systems (Fig. 5d and e) and the tilt angle was almost always more than 75° (Fig. 5f). Shifting from a horizontal to a vertical state was explained by the electrostatic interactions between the functionalized CNT and lipid bilayer (Fig. 5e). The number of hydrogen bonds formed between hydroxyl groups on the ends of functionalized CNT and lipid headgroups was an average of about 5 which led them to complicated with each other, and functionalized CNT was prone to vertical orientation (Fig. 5g). Liu and coworkers[137] used nonequilibrium MDS to explore methane diffusion through (10,10) CNT membranes at 300 K and up to 15 bar, highlighting the significant role of interfacial

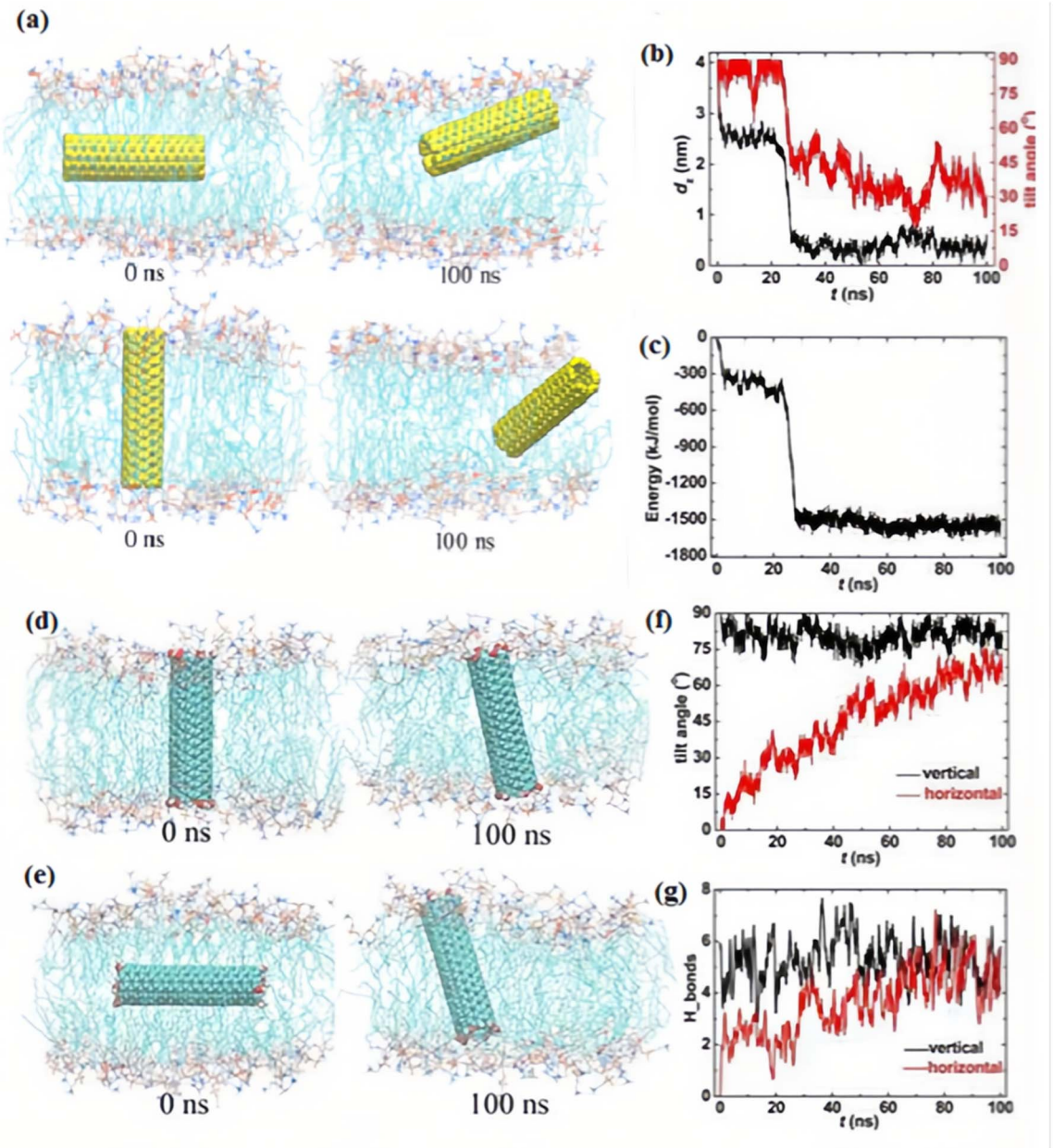

Fig. 5 An entering route of pure CNT and functionalized CNT situated in the membrane vertically and horizontally. (a) Snapshots at critical times for pure CNT. (b and c) Time evolvement of the center of mass (COM) distance in the z-direction, the tilt angle, and the interaction energy between pure CNT and membrane. (d and e) Snapshots at $t = 0$ ns and 100 ns for functionalized CNT, (f) the tilt angle, and (g) the hydrogen bonds between functionalized CNT and lipid bilayer membrane. Figure reproduce with permission from ref. 39. Copyright 2019, Multidisciplinary Digital Publishing Institute (MDPI).

resistance at CNT entrances and exits in reducing permeability by over two orders of magnitude.[137] They[137] found that factors such as the adsorption affinity and surface area of the surrounding matrix (flanges) greatly influence transport performance. Their model distinguishes between flange resistance and entrance–exit resistance, emphasizing how membrane porosity and surface interactions independently regulate mass transfer.[137] These insights provide a deeper mechanistic understanding of how CNT geometry and surface chemistry affect diffusion efficiency in nanostructured membranes.[137] Li and coworkers [138] introduced boron nitride nanotube porins (BNNTPs) as synthetic membrane channels that closely mimic biological porins, with diameters around 2 nm and high ion transport efficiency.[138] Using cryo-TEM, DNA translocation, and liposome assays, they demonstrated successful BNNTP integration into lipid bilayers. Notably, BNNTPs exhibited strong cation selectivity, unusual $C^{1}/^{4}$ scaling with ion concentration, and pH-dependent conductance. Their osmotic energy harvesting experiments revealed exceptional

power densities (up to 12 kW m^{-2}), greatly outperforming previous BNNT-based systems.[138]

7. Conclusion

In this review, we examined the potential of carbon nanotubes (CNTs) in designing transmembrane channels to enhance the mass transfer through the cells' lipid bilayer membrane. Our analysis highlighted the significance of the CNT length, noting that while shorter CNTs can serve as stable membrane channels, longer CNTs tend to become obstructed within the hydrophobic regions of the cell membrane. This insight underscored the importance of optimizing CNT length for effective membrane integration. Furthermore, we explored the impact of surface functionalization on CNT permeability. The previous research results indicated that pure CNTs can readily penetrate plasma membranes without specific orientations, often causing membrane disruption. In contrast, functionalized CNTs demonstrated a preference for vertical alignment, which minimized membrane damage and reduces energy barriers. The density and type of functional groups, such as carboxylic and amine groups, played a crucial role in maintaining this vertical orientation and ensuring stable insertion into lipid membranes. The study concludes that functionalized CNTs, with their ability to maintain vertical configurations and reduce membrane perturbation, are proper candidates for acting as synthetic channels in the cell membrane. To overcome current barriers in the practical application of CNT-based membrane channels, future research should also prioritize the integration of CNTs with living systems by improving biocompatibility and minimizing cytotoxicity, which can be achieved through advanced surface functionalization and biomimetic coatings. Moreover, scalable and reproducible fabrication techniques need to be developed to enable large-scale production of uniform CNT channels with controlled length and functionalization patterns. Finally, exploring responsive gating mechanisms, such as stimuli-responsive functional groups or external control *via* electric or optical signals, could provide dynamic regulation of channel permeability, enhancing their utility in smart drug delivery and biosensing applications. Addressing these challenges will be critical for translating CNT membrane channels from laboratory studies to real-world biomedical and environmental technologies. In summary, the strategic functionalization of CNTs presents a promising approach to developing effective membrane channels, paving the way for advanced innovations in biomedical, environmental and engineering applications. Future research should mainly focus on optimizing functional group characteristics and densities to further enhance the efficacy and safety of CNT-based membrane channels in various applications.

Data availability

No primary research results, software or code have been included and no new data were generated or analysed as part of this review.

Author contributions

Sara Yazdani: data curation, writing – original draft, conceptualization, supervision, project administration, writing – review &editing. Davoud Biria: supervision, project administration, writing – review &editing. Gholamreza Pazuki: data curation, writing – original draft, writing – review & editing.

Conflicts of interest

There are no conflicts to declare.

Acknowledgements

The authors would like to thank the Iran National Science Foundation (INSF) and University of Isfahan for funding this work, through the grant no. 4014348.

References

1 E. D. Korn, *Annu. Rev. Biochem.*, 1969, **38**, 263–288.
2 R. A. Gatenby, *Int. J. Mol. Sci.*, 2019, **20**, 3609.
3 S. M. Zargar, D. K. Hafshejani, A. Eskandarinia, M. Rafienia and A. Z. Kharazi, *J. Med. Signals Sens.*, 2019, **9**, 181–189.
4 S. Tan, T. Wu, D. Zhang and Z. Zhang, *Theranostics*, 2015, **5**, 863.
5 C. Dai, Q. Xu, L. Li, Y. Liu and S. Qu, *ACS Biomater. Sci. Eng.*, 2024, **10**, 1988–2000.
6 S. Yazdani, S. M. Ghoreishi and N. Habibi, *Protein Pept. Lett.*, 2022, **29**, 80–88.
7 K. Niikura, K. Nambara, T. Okajima, Y. Matsuo and K. Ijiro, *Langmuir*, 2010, **26**, 9170–9175.
8 B. R. Liu, S.-H. Chiou, Y.-W. Huang and H.-J. Lee, *Membranes*, 2022, **12**, 88.
9 K. Kardani, A. Milani, S. H. Shabani and A. Bolhassani, *Expet Opin. Drug Deliv.*, 2019, **16**, 1227–1258.
10 M. Hao, L. Zhang and P. Chen, *Int. J. Mol. Sci.*, 2022, **23**, 9038.
11 E. Böhmová, D. Machová, M. Pechar, R. Pola, K. Venclíková, O. Janoušková and T. Etrych, *Physiol. Res.*, 2018, **67**, S267–S279.
12 F. Wahid, T. Khan, A. Shehzad, M. Ul-Islam and Y. Kim, *J. Nanosci. Nanotechnol.*, 2014, **14**, 744–754.
13 A. Verma, O. Uzun, Y. Hu, Y. Hu, H.-S. Han, N. Watson, S. Chen, D. J. Irvine and F. Stellacci, *Nat. Mater.*, 2008, **7**, 588–595.
14 M. Zhu, G. Nie, H. Meng, T. Xia, A. Nel and Y. Zhao, *Accounts Chem. Res.*, 2013, **46**, 622–631.
15 J. H. Lee, H.-S. Kim, E.-T. Yun, S.-Y. Ham, J.-H. Park, C. H. Ahn, S. H. Lee and H.-D. Park, *Membranes*, 2020, **10**, 273.
16 M. Barrejón and M. Prato, *Adv. Mater. Interfaces*, 2022, **9**, 2101260.
17 C. Corredor, W.-C. Hou, S. A. Klein, B. Y. Moghadam, M. Goryll, K. Doudrick, P. Westerhoff and J. D. Posner, *Carbon*, 2013, **60**, 67–75.
18 R. Shoukat and M. I. Khan, *Microsyst. Technol.*, 2021, 1–10.

19 A. Kohls, M. Maurer Ditty, F. Dehghandehnavi and S.-Y. Zheng, *ACS Appl. Mater. Interfaces*, 2022, **14**, 6287–6306.
20 F. Alber, S. Dokudovskaya, L. M. Veenhoff, W. Zhang, J. Kipper, D. Devos, A. Suprapto, O. Karni-Schmidt, R. Williams and B. T. Chait, *Nature*, 2007, **450**, 695–701.
21 M. A. Dobrovolskaia and S. E. McNeil, *Nat. Nanotechnol.*, 2007, **2**, 469–478.
22 J. Chen, S. Wei and H. Xie, *J. Phys.:Conf. Ser.*, 2021, **1948**, 012184.
23 Y. Fu, *ChemistrySelect*, 2022, **7**, e202103222.
24 R. Maheswaran and B. P. Shanmugavel, *J. Electron. Mater.*, 2022, **51**, 2786–2800.
25 T. V. Patil, D. K. Patel, S. D. Dutta, K. Ganguly, A. Randhawa and K.-T. Lim, *Appl. Sci.*, 2021, **11**, 9550.
26 J. Simon, E. Flahaut and M. Golzio, *Materials*, 2019, **12**, 624.
27 R. Jha, A. Singh, P. Sharma and N. K. Fuloria, *J. Drug Delivery Sci. Technol.*, 2020, **58**, 101811.
28 S. Yazdani, M. Mozaffarian, G. Pazuki, N. Hadidi, I. Villate-Beitia, J. Zárate, G. Puras and J. L. Pedraz, *Pharmaceutics*, 2024, **16**, 288.
29 M. I. Sajid, U. Jamshaid, T. Jamshaid, N. Zafar, H. Fessi and A. Elaissari, *Int. J. Pharm.*, 2016, **501**, 278–299.
30 S. Yazdani, M. Mozaffarian, G. Pazuki and N. Hadidi, *Cell. Signal.*, 2024, **2**, 148–154.
31 S. K. Debnath and R. Srivastava, *Front. Nanotechnol.*, 2021, **3**, 644564.
32 M. R. Chetyrkina, F. S. Fedorov and A. G. Nasibulin, *RSC Adv.*, 2022, **12**, 16235–16256.
33 L. Tang, Q. Xiao, Y. Mei, S. He, Z. Zhang, R. Wang and W. Wang, *J. Nanobiotechnol.*, 2021, **19**, 1–28.
34 L. Lacerda, H. Ali-Boucetta, S. Kraszewski, M. Tarek, M. Prato, C. Ramseyer, K. Kostarelos and A. Bianco, *Nanoscale*, 2013, **5**, 10242–10250.
35 P. Ghoderao, S. Sahare, P. Alegaonkar, A. A. Kulkarni and T. Bhave, *ACS Appl. Nano Mater.*, 2018, **2**, 607–616.
36 J. M. Tan, S. Bullo, S. Fakurazi and M. Z. Hussein, *Polymers*, 2021, **13**, 1362.
37 M. E. David, R. M. Ion, R. M. Grigorescu, L. Iancu, A. M. Holban, F. Iordache, A. I. Nicoara, E. Alexandrescu, R. Somoghi and S. Teodorescu, *Nanomaterials*, 2022, **12**, 239.
38 A. Khalid, A. Madni, B. Raza, M. ul Islam, A. Hassan, F. Ahmad, H. Ali, T. Khan and F. Wahid, *Int. J. Biol. Macromol.*, 2022, **203**, 256–267.
39 Y. Gao, D. Mao, J. Wu, X. Wang, Z. Wang, G. Zhou, L. Chen, J. Chen and S. Zeng, *Appl. Sci.*, 2019, **9**, 4271.
40 B. Huang, *Biomanufacturing Reviews*, 2020, **5**, 3.
41 J. Liao, H. Wang, N. Liu and H. Yang, *Adv. Colloid Interface Sci.*, 2023, **311**, 102812.
42 S. Yazdani, M. Mozaffarian, G. Pazuki and N. Hadidi, *J. Mol. Liq.*, 2022, **360**, 119519.
43 R. Alshehri, A. M. Ilyas, A. Hasan, A. Arnaout, F. Ahmed and A. Memic, *J. Med. Chem.*, 2016, **59**, 8149–8167.
44 A. Brandelli, *Food Sci. Hum. Wellness*, 2020, **9**, 8–20.
45 R. Abbasi, G. Shineh, M. Mobaraki, S. Doughty and L. Tayebi, *J. Nanopart. Res.*, 2023, **25**, 43.
46 C. A. Poland, R. Duffin, I. Kinloch, A. Maynard, W. A. Wallace, A. Seaton, V. Stone, S. Brown, W. MacNee and K. Donaldson, *Nat. Nanotechnol.*, 2008, **3**, 423–428.
47 A. Abdal Dayem, M. K. Hossain, S. B. Lee, K. Kim, S. K. Saha, G.-M. Yang, H. Y. Choi and S.-G. Cho, *Int. J. Mol. Sci.*, 2017, **18**, 120.
48 N. Sharma, B. D. Kurmi, D. Singh, S. Mehan, K. Khanna, R. Karwasra, S. Kumar, A. Chaudhary, V. Jakhmola and A. Sharma, *J. Drug Targeting*, 2024, 1–13.
49 Q. Liu and M. W. Urban, *Polym. Rev.*, 2023, **63**, 289–323.
50 A. Di Crescenzo, V. Ettorre and A. Fontana, *Beilstein J. Nanotechnol.*, 2014, **5**, 1675–1690.
51 M. Assali, N. Kittana, S. Alhaj-Qasem, M. Hajjyahya, H. Abu-Rass, W. Alshaer and R. Al-Buqain, *Sci. Rep.*, 2022, **12**, 12062.
52 L. Lavagna, R. Nisticò, S. Musso and M. Pavese, *Mater. Today Chem.*, 2021, **20**, 100477.
53 M. Karimi, A. Ghasemi, S. Mirkiani, M. M. Basri and M. Hamblin, *Carbon Nanotubes in Drug and Gene Delivery*, Morgan & Claypool Publishers, 2017.
54 M. Luo, P. Chen, J. Wang, X. Deng, L. Dong, M. Wu and X. Shen, *Sci. China Chem.*, 2016, **59**, 918–926.
55 T. Wen, A. Yang, L. Piao, S. Hao, L. Du, J. Meng, J. Liu and H. Xu, *Int. J. Nanomed.*, 2019, 4475–4489.
56 J. Long, W. Ma, Z. Yu, H. Liu and Y. Cao, *Nanotoxicology*, 2019, **13**, 938–951.
57 H. Yang, J. Li, C. Yang, H. Liu and Y. Cao, *Toxicol. Appl. Pharmacol.*, 2019, **374**, 11–19.
58 V. Vijayalakshmi, B. Sadanandan and A. V. Raghu, *Results Chem.*, 2022, **4**, 100484.
59 G. Visalli, A. Facciolà, D. Iannazzo, A. Piperno, A. Pistone and A. Di Pietro, *J. Trace Elem. Med. Biol.*, 2017, **43**, 153–160.
60 H.-B. Kim, B. Jin, D. K. Patel, J.-W. Kim, J. Kim, H. Seonwoo and K.-T. Lim, *IEEE Trans. NanoBioscience*, 2019, **18**, 463–468.
61 X. Zhao, S. Chang, J. Long, J. Li, X. Li and Y. Cao, *Food Chem. Toxicol.*, 2019, **126**, 169–177.
62 T. Jiang, C. A. Amadei, N. Gou, Y. Lin, J. Lan, C. D. Vecitis and A. Z. Gu, *Environ. Sci.: Nano*, 2020, **7**, 1348–1364.
63 A. Chowdhry, J. Kaur, M. Khatri, V. Puri, R. Tuli and S. Puri, *Heliyon*, 2019, **5**(10), e02605.
64 S. Yazdani, M. Mozaffarian, G. Pazuki, N. Hadidi, I. Gallego, G. Puras and J. L. Pedraz, *Sci. Rep.*, 2022, **12**, 21114.
65 J. Du, S. Wang, H. You and X. Zhao, *Environ. Toxicol. Pharmacol.*, 2013, **36**, 451–462.
66 K. Aschberger, H. J. Johnston, V. Stone, R. J. Aitken, S. M. Hankin, S. A. Peters, C. L. Tran and F. M. Christensen, *Crit. Rev. Toxicol.*, 2010, **40**, 759–790.
67 G. Bode, *Drug discovery and evaluation: Methods in clinical Pharmacology*, 2020, pp. 1085–1138.
68 G. Bode, P. Starck-Lantova and P.-J. Kramer, in *Drug Discovery and Evaluation: Safety and Pharmacokinetic Assays*, Springer, 2023, pp. 1–26.
69 K. R. Santhanakrishnan, J. Koilpillai, D. Narayanasamy and K. Santhanakrishnan, *Cureus*, 2024, 16.
70 P. Sengupta, in *Antibacterial and Antiviral Functional Materials*, ACS Publications, 2024, vol. 2, pp. 361–401.

71 B. Rezaei, A. Harun, X. Wu, P. R. Iyer, S. Mostufa, S. Ciannella, I. H. Karampelas, J. Chalmers, I. Srivastava and J. Gómez-Pastora, *Adv. Healthcare Mater.*, 2024, **13**, 2401213.
72 L. Sonowal and S. Gautam, *Nano-Struct. Nano-Objects*, 2024, **38**, 101117.
73 N. Elahi and C. D. Zeinalipour-Yazdi, *C*, 2025, **11**, 35.
74 J. Yu, S. Liu, B. Wu, Z. Shen, G. N. Cherr, X.-X. Zhang and M. Li, *Environ. Sci. Technol.*, 2016, **50**, 3985–3994.
75 P. Zhao, L. Chen, H. Shao, Y. Zhang, Y. Sun, Y. Ke, S. Ramakrishna, L. He and W. Xue, *Biomed. Mater.*, 2016, **11**, 015021.
76 M. Yu, R. Chen, Z. Jia, J. Chen, J. Lou, S. Tang and X. Zhang, *Int. J. Toxicol.*, 2016, **35**, 17–26.
77 L.-C. Ong, Y.-F. Tan, B. S. Tan, F. F.-L. Chung, S.-K. Cheong and C.-O. Leong, *Toxicol. Appl. Pharmacol.*, 2017, **329**, 347–357.
78 J. Long, Y. Xiao, L. Liu and Y. Cao, *J. Nanobiotechnol.*, 2017, **15**, 1–13.
79 O. M. Perepelytsina, A. P. Ugnivenko, A. V. Dobrydnev, O. N. Bakalinska, A. I. Marynin and M. V. Sydorenko, *Nanoscale Res. Lett.*, 2018, **13**, 1–16.
80 N. Lu, Y. Sui, R. Tian and Y.-Y. Peng, *Chem. Res. Toxicol.*, 2018, **31**, 1061–1068.
81 N. Lu, Y. Sui, Y. Ding, R. Tian, L. Li and F. Liu, *Chem. Biol. Interact.*, 2018, **295**, 64–72.
82 F. Valentini, E. Mari, A. Zicari, A. Calcaterra, M. Talamo, M. G. Scioli, A. Orlandi and S. Mardente, *Int. J. Mol. Sci.*, 2018, **19**, 1316.
83 S. Fiorito, J. Russier, A. Salemme, M. Soligo, L. Manni, E. Krasnowska, S. Bonnamy, E. Flahaut, A. Serafino and G. I. Togna, *Carbon*, 2018, **129**, 572–584.
84 Y. Sun, J. Gong and Y. Cao, *Int. J. Nanomed.*, 2019, 9285–9294.
85 R. J. Snyder, K. C. Verhein, H. L. Vellers, A. B. Burkholder, S. Garantziotis and S. R. Kleeberger, *Nanotoxicology*, 2019, **13**, 1344–1361.
86 K.-C. Lee, P.-Y. Lo, G.-Y. Lee, J.-H. Zheng and E.-C. Cho, *J. Biotechnol.*, 2019, **296**, 14–21.
87 O. Sabido, A. Figarol, J.-P. Klein, V. Bin, V. Forest, J. Pourchez, B. Fubini, M. Cottier, M. Tomatis and D. Boudard, *Nanomaterials*, 2020, **10**, 319.
88 S. M. Reamon-Buettner, A. Hackbarth, A. Leonhardt, A. Braun and C. Ziemann, *Mech. Ageing Dev.*, 2021, **193**, 111412.
89 K. Kyriakidou, D. Brasinika, A. Trompeta, E. Bergamaschi, I. Karoussis and C. Charitidis, *Food Chem. Toxicol.*, 2020, **141**, 111374.
90 J. Czarnecka, M. Wiśniewski, N. Forbot, P. Bolibok, A. P. Terzyk and K. Roszek, *Materials*, 2020, **13**, 2060.
91 K. Fraser, V. Kodali, N. Yanamala, M. E. Birch, L. Cena, G. Casuccio, K. Bunker, T. L. Lersch, D. E. Evans and A. Stefaniak, *Part. Fibre Toxicol.*, 2020, **17**, 1–26.
92 J. A. Uribe-Calderon, C. G. Poot-Bote, J. M. Cervantes-Uc, E. L. Pacheco-Pantoja, I. Echevarría-Machado and N. Rodríguez-Fuentes, *J. Nanopart. Res.*, 2022, **24**, 151.
93 V. Vijayalakshmi, B. Sadanandan and R. V. Anjanapura, *J. Biochem. Mol. Toxicol.*, 2023, **37**, e23283.
94 S. Zhang, J. Li, G. Lykotrafitis, G. Bao and S. Suresh, *Adv. Mater.*, 2009, **21**, 419.
95 A. Chaudhuri, G. Battaglia and R. Golestanian, *Phys. Biol.*, 2011, **8**, 046002.
96 K. Yang, B. Yuan and Y.-q. Ma, *Nanoscale*, 2013, **5**, 7998–8006.
97 L. Chen, S. Xiao, H. Zhu, L. Wang and H. Liang, *Soft Matter*, 2016, **12**, 2632–2641.
98 J. Mao, P. Chen, J. Liang, R. Guo and L.-T. Yan, *ACS Nano*, 2016, **10**, 1493–1502.
99 D. M. Richards and R. G. Endres, *Proc. Natl. Acad. Sci. U.S.A.*, 2016, **113**(22), 6113–6118.
100 Y. Zheng, H. Tang, H. Ye and H. Zhang, *RSC Adv.*, 2015, **5**, 43772–43779.
101 H. Tang, H. Zhang, H. Ye and Y. Zheng, *J. Appl. Phys.*, 2016, **120**(1121), 114701.
102 H. Tang, H. Zhang, H. Ye and Y. Zheng, *J. Phys. Chem. B*, 2018, **122**, 171–180.
103 K. Deng, Z. Luo, L. Tan and Z. Quan, *Chem. Soc. Rev.*, 2020, **49**, 6002–6038.
104 H. Ijaz, A. Mahmood, M. M. Abdel-Daim, R. M. Sarfraz, M. Zaman, N. Zafar, S. Alshehery, M. M. Salem-Bekhit, M. A. Ali and L. B. Eltayeb, *Inorg. Chem. Commun.*, 2023, **155**, 111020.
105 O. Akturk, in *Handbook of Functionalized Carbon Nanostructures: from Synthesis Methods to Applications*, Springer, 2024, pp. 2657–2699.
106 S. Das, S. Roy, S. C. Dinda, A. Bose, C. Mahapatra, B. Basu and B. Prajapati, *Results Chem.*, 2025, 102206.
107 G. Ciofani, V. Raffa, A. Menciassi and A. Cuschieri, *Biotechnol. Bioeng.*, 2008, **101**, 850–858.
108 K. Kostarelos, L. Lacerda, G. Pastorin, W. Wu, S. Wieckowski, J. Luangsivilay, S. Godefroy, D. Pantarotto, J.-P. Briand and S. Muller, *Nat. Nanotechnol.*, 2007, **2**, 108–113.
109 N. W. Shi Kam, T. C. Jessop, P. A. Wender and H. Dai, *J. Am. Chem. Soc.*, 2004, **126**, 6850–6851.
110 V. Raffa, G. Ciofani, S. Nitodas, T. Karachalios, D. D'Alessandro, M. Masini and A. Cuschieri, *Carbon*, 2008, **46**, 1600–1610.
111 C. Shen, G. Zou, W. Guo and H. Gao, *Carbon*, 2020, **164**, 391–397.
112 M. Lepoitevin, T. Ma, M. Bechelany, J.-M. Janot and S. Balme, *Adv. Colloid Interface Sci.*, 2017, **250**, 195–213.
113 J.-M. Pagès, C. E. James and M. Winterhalter, *Nat. Rev. Microbiol.*, 2008, **6**, 893–903.
114 J. Geng, K. Kim, J. Zhang, A. Escalada, R. Tunuguntla, L. R. Comolli, F. I. Allen, A. V. Shnyrova, K. R. Cho and D. Munoz, *Nature*, 2014, **514**, 612–615.
115 M. N. Norizan, M. H. Moklis, S. Z. N. Demon, N. A. Halim, A. Samsuri, I. S. Mohamad, V. F. Knight and N. Abdullah, *RSC Adv.*, 2020, **10**, 43704–43732.
116 V. Pérez-Luna, C. Moreno-Aguilar, J. L. Arauz-Lara, S. Aranda-Espinoza and M. Quintana, *Sci. Rep.*, 2018, **8**, 17998.

117 K. Sullivan, Y. Zhang, J. Lopez, M. Lowe and A. Noy, *Sci. Rep.*, 2020, **10**, 11908.
118 R. H. Tunuguntla, A. Escalada, V. A. Frolov and A. Noy, *Nat. Protoc.*, 2016, **11**, 2029–2047.
119 N. T. Ho, M. Siggel, K. V. Camacho, R. M. Bhaskara, J. M. Hicks, Y.-C. Yao, Y. Zhang, J. Köfinger, G. Hummer and A. Noy, *Proc. Natl. Acad. Sci. U.S.A.*, 2021, **118**, e2016974118.
120 D. Liu, Y. Mao and L. Ding, *J. Water Health*, 2018, **16**, 171–180.
121 Y. Li, Z. Li, F. Aydin, J. Quan, X. Chen, Y.-C. Yao, C. Zhan, Y. Chen, T. A. Pham and A. Noy, *Sci. Adv.*, 2020, **6**, eaba9966.
122 J. Chen, G. Zhou, L. Chen, Y. Wang, X. Wang and S. Zeng, *J. Phys. Chem. C*, 2016, **120**, 6225–6231.
123 G. Gul, R. Faller and N. Ileri-Ercan, *Biophys. J.*, 2023, **122**, 1748–1761.
124 M. Vögele, J. Köfinger and G. Hummer, *Faraday Discuss.*, 2018, **209**, 341–358.
125 C. F. Lopez, S. O. Nielsen, P. B. Moore and M. L. Klein, *Proc. Natl. Acad. Sci. U.S.A.*, 2004, **101**, 4431–4434.
126 U. Zimmerli and P. Koumoutsakos, *Biophys. J.*, 2008, **94**, 2546–2557.
127 S. Höfinger, M. Melle-Franco, T. Gallo, A. Cantelli, M. Calvaresi, J. A. Gomes and F. Zerbetto, *Biomaterials*, 2011, **32**, 7079–7085.
128 A. Ben-Shaul, I. Szleifer and W. Gelbart, *J. Chem. Phys.*, 1985, **83**, 3597–3611.
129 S. Pogodin and V. A. Baulin, *ACS Nano*, 2010, **4**, 5293–5300.
130 S. Pogodin, N. K. Slater and V. A. Baulin, *ACS Nano*, 2011, **5**, 1141–1146.
131 S. Pogodin and V. A. Baulin, *Soft Matter*, 2010, **6**, 2216–2226.
132 S. Kraszewski, A. Bianco, M. Tarek and C. Ramseyer, *PLoS One*, 2012, **7**, e40703.
133 P. Raczyński, K. Gorny, M. Pabiszczak and Z. Gburski, *Comput. Mater. Sci.*, 2013, **70**, 13–18.
134 S. Baoukina, L. Monticelli and D. P. Tieleman, *J. Phys. Chem. B*, 2013, **117**, 12113–12123.
135 S. Kraszewski, F. Picaud, I. Elhechmi, T. Gharbi and C. Ramseyer, *Carbon*, 2012, **50**, 5301–5308.
136 S. Tabari, Y. Jamali and R. Poursalehi, *Procedia Mater. Sci.*, 2015, **11**, 423–427.
137 L. Liu, D. Nicholson and S. K. Bhatia, *ACS Appl. Mater. Interfaces*, 2018, **10**, 34706–34717.
138 Z. Li, A. T. Hall, Y. Wang, Y. Li, D. O. Byrne, L. R. Scammell, R. R. Whitney, F. I. Allen, J. Cumings and A. Noy, *Sci. Adv.*, 2024, **10**, eado8081.